Final Technical Report
Earthquake Hazards Program Assistance Awards

USGS Award Number: G11AP20136, G11AP20138 and G11AP20142

Development of a Holocene earthquake record for the northern San Jacinto Fault zone from a new paleoseismic site at Mystic Lake: Collaborative Research with CSULB, SDSU, and CSUSB.

Nate Onderdonk Dept. of Geological Sciences, CSU Long Beach
1250 Bellflower Blvd. Long Beach, CA 90840 P: 562-895-2654, F: 562-985-8638
nonderdo@csulb.edu

Thomas K. Rockwell Dept. of Geological Sciences, San Diego State University
San Diego, CA 92182 P: 619-594-4441, F: 619-594-4372
trockwell@geology.sdsu.edu

Sally McGill Department of Geological Sciences CSU, San Bernardino
San Bernardino, CA 92407 P: 909-537-5347 F: 909-537-5118
smcgill@csusb.edu

Term covered by this report: May 1, 2012 to April 30, 2014

Abstract
Paleoseismic trenching at the Mystic Lake site has resulted in a record of 15 earthquakes over the past 3700 years on the Claremont fault segment of the northern San Jacinto fault zone. We believe we have a complete record for the past 2000 years during which there were 11 or 12 earthquakes. Our record for the preceding 1700 years (0 to 1700 BC) only includes 3 or 4 earthquakes and is most likely not complete due to missing stratigraphic section. The recurrence interval for the last 2000 years is between 160 and 190 years, and the last ground rupturing earthquake occurred around 1800 AD. The 214 years that have passed since the last rupture is equal or slightly larger than the longest hiatuses between earthquakes in the past 2000 years, suggesting the fault may be near the end of its earthquake cycle.

Purpose and significance of study
The purpose of this project was to obtain a record of earthquakes for the past 4000 years on the northern San Jacinto fault where no paleoseismic data previously existed. With the granted funds, as well as supplemental funding from the Southern California Earthquake Center, we were able to excavate trenches to a depth of 6 m, which corresponds to the past 3700 years at the Mystic Lake site (Figure 1). These trenches exposed evidence for 15 earthquakes, 12 of which occurred in the past 2000 years. This new paleoseismic record from the Claremont segment of the northern San Jacinto fault zone has enabled us to:

1. estimate the probability of future large earthquakes based on the patterns of earthquake recurrence on the fault and the timing of the last ground-rupturing earthquake.
2. evaluate the possibility of earthquakes rupturing through the step-overs at either end of the Claremont fault by comparing the timing of events on the Claremont fault to the timing of events on the Clark fault to the south, and the Mojave segment of the San Andreas fault to the north.
3. estimate the average size of ground-rupturing earthquakes based on the number of events in the past 2000 years and the slip-rate of the fault from coeval work along the Claremont fault.

Methods
This study relied on excavation of trenches across the Claremont fault at the Mystic Lake site to expose evidence of past surface ruptures along the fault. The site was first identified in 2007 using field mapping aided by .5 m resolution Digital Elevation Models constructed using the B4 LiDAR dataset (Bevis et al., 2006). In 2009, several trenches were excavated at the site to precisely locate the primary fault strand and evaluate the relative activity of the three fault strands that were identified in the topography. Three of these trenches were excavated across obvious scarps, and the fourth was a 400 m long, 2 m deep trench excavated across the full length of a sag that had been identified on a 1940 air photo (Figure 2). The exposures in these trenches enabled us to recognize the location of the primary fault strand and collect paleoseismic data from all three fault strands at the site. In 2010, three additional shallow (2 m deep) trenches were excavated along the main fault strand, exposing additional evidence for the events seen in 2009 and refining the ages for the most recent 7 earthquake ruptures through the site. The funding provided by this grant was used to confirm these last 7 earthquakes and extend the record back to almost 4000 years with deeper trenches over two field seasons. In 2012, a deeper

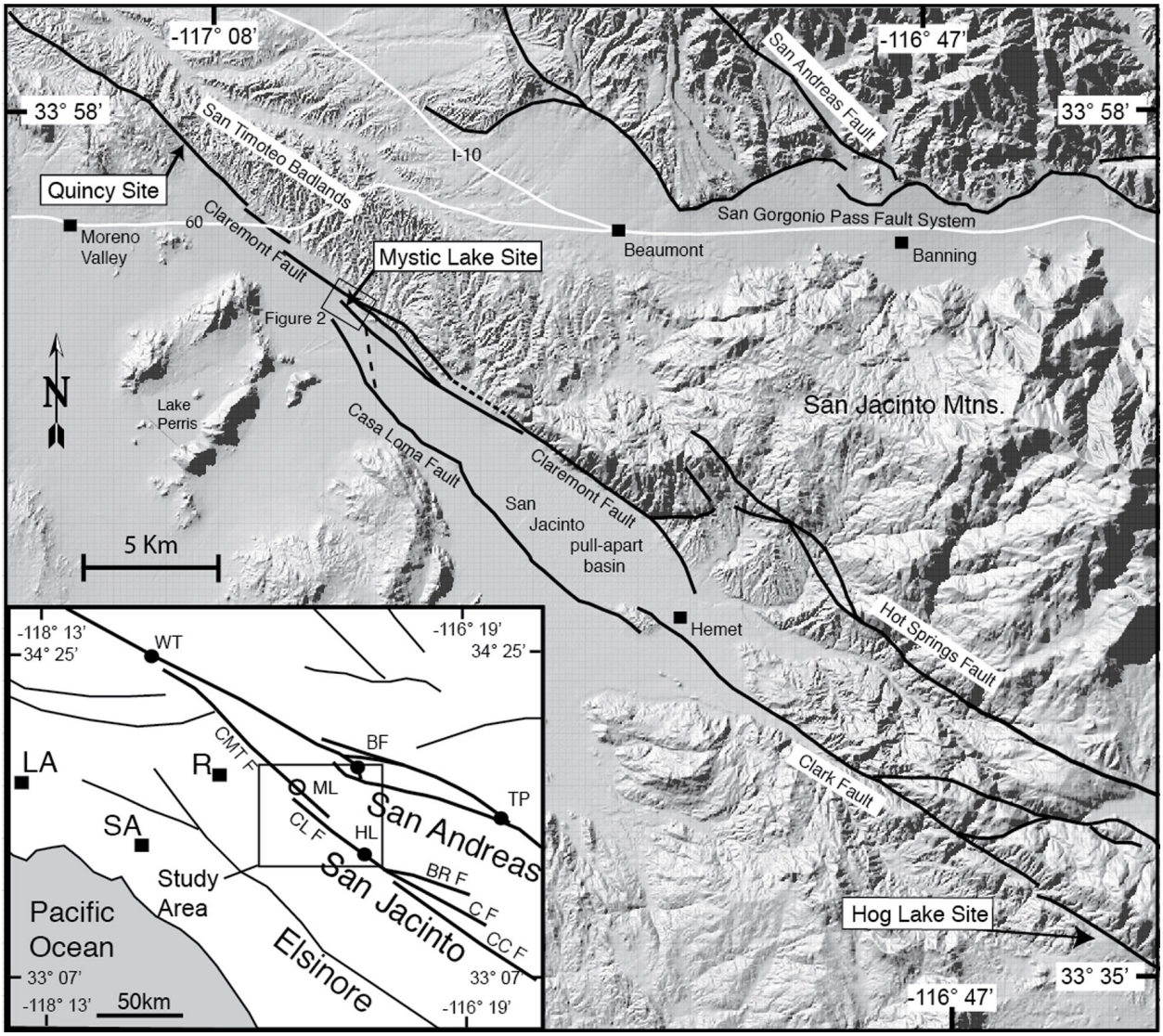

Figure 1. Digital elevation model of the southern Claremont fault showing faults (black lines) and pertinent locations and topographic features. Inset map shows the southern San Andreas fault system with selected paleoseismic sites shown as black circles. WT= Wrightwood, BF= Burro Flats, TP= Thousand Palms, ML= Mystic Lake, HL= Hog Lake. Faults include the Claremont fault (CMT F), Casa Loma fault (CL F), Clark fault (C F), Buck Ridge fault (BR F) and the Coyote Creek fault (CC F).

(4.5 m deep) trench was excavated to expose older sediments along the main fault zone and provided evidence for 11 events on the main fault strand during the past 2000 years. In 2013, a second deeper and wider trench was excavated in the same location as the 2012 trench. This trench was 6 m deep and provided evidence for a total of 15 earthquakes in the past 3700 years.

All trench exposures were evaluated and documented using the same methodology. Trenches were excavated using a backhoe or excavator and trench walls were then scraped and cleaned by hand. A string grid was set up on the trench walls to divide the exposure into 1 m wide by .5 m

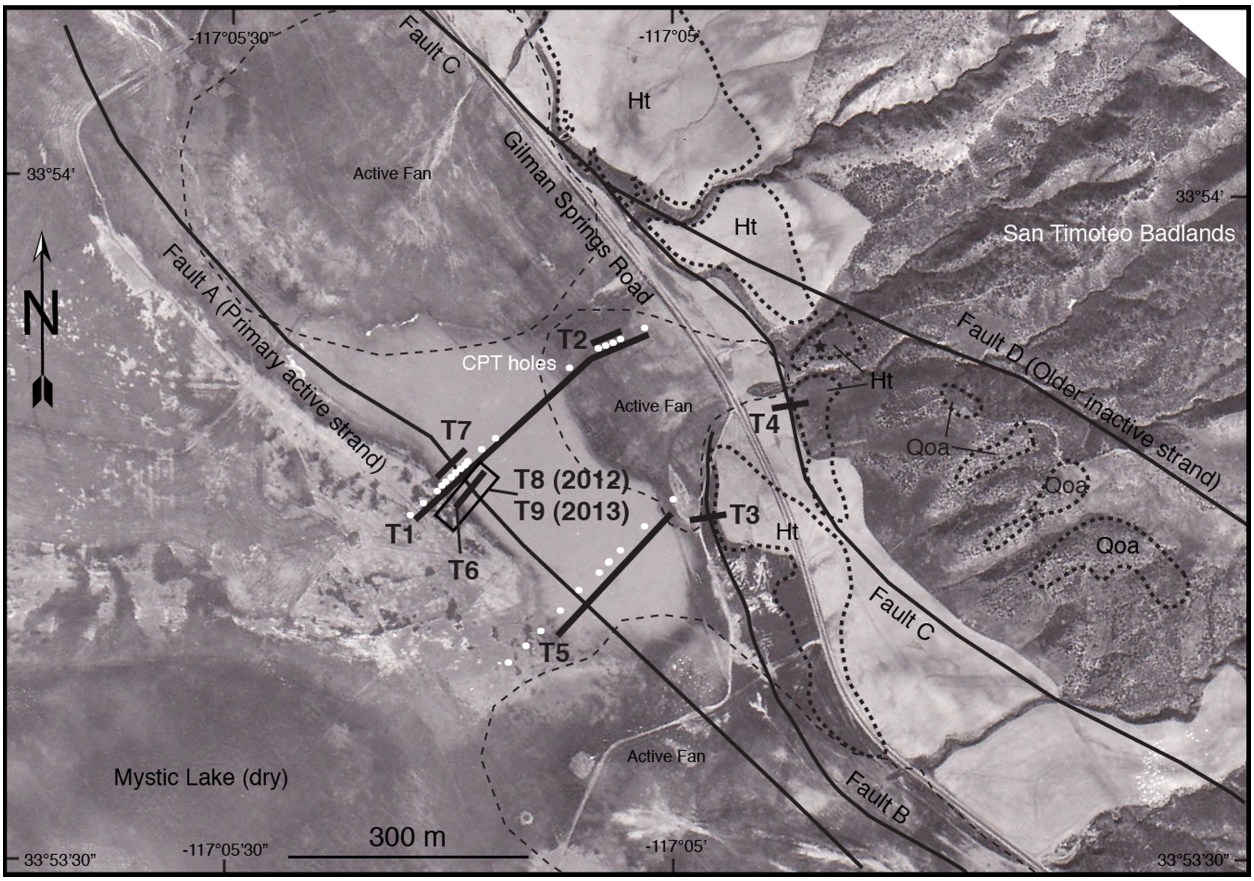

Figure 2. 1940 air photo of the Mystic Lake site with faults (thin black lines), trenches (thicker black lines), CPT holes (white dots), and selected Quaternary deposits. Note the water that is ponded behind Fault A and roughly defines the sag between Faults A, B, and C.

tall panels. Stratigraphic units were identified, named, traced, and correlated across the trench and between separate trenches. Stratigraphic and structural relationships were identified and described and any datable material was collected, cataloged, and the locations marked on the trench walls. All trench panels were photographed and then digitally assembled into mosaics. The stratigraphic and structural relationships were then drawn on the printed photo logs in the field. Members of the SCEC community and other local experts were invited each year to observe the open trench(s), and to critique and discuss our interpretations of the relationships exposed in the trench walls.

Over 700 samples were collected for radiocarbon dating from the nine trenches. 118 of these were dated at the Keck Carbon Cycle Accelerator Mass Spectrometry Program at the University of California, Irvine (Appendix 1). 45 samples were charged to this grant, the rest were funded by multiple grants from the Southern California Earthquake Center. The dates were evaluated with respect to their stratigraphic position and the other dates and several models of the ages of stratigraphic units were proposed and evaluated. Because most of the samples were detrital charcoal, there is an unknown amount of time between the growth of the wood, the formation of the charcoal during a brush fire, and the deposition of the charcoal in the Mystic Lake stratigraphy. Consequently, a layer is most likely younger than the charcoal it contains and the

youngest charcoal age from each layer is assumed to provide the closest approximation of the age of that layer. Using this logic, and the assumption that radiocarbon samples with older ages than underlying units do not represent the true age of the unit they are in, we eliminated almost half of the dated samples from our preferred stratigraphic model, which used a total of 70 samples. An event history for the site was then determined using OxCal software (Bronk Ramsey, 2009), which calculates the probability density functions (PDFs) of radiocarbon sample ages and the event ages based on the dendro-chronologically calibrated radiocarbon curve of Reimer et al. (2009).

Results

Site description

The Mystic Lake site is a 300 m wide by 500 m long sag that has formed between strands of the Claremont fault at the north end of Mystic Lake (Figure 1, 2). Mystic lake is an ephemeral lake that fills the lowest elevations of a pull-apart basin between the Claremont and Casa Loma faults during wet years. There are four strands of the Claremont fault that pass through the site. Geomorphic observations and trenching indicates that the southwest strand (Fault A) is the primary strand although it has no present-day geomorphic expression due to continued deposition in the sag. In air photos from the 1940's, a small depression is visible on the northeast side of Fault A that does not exist today. In Trench 1, the youngest unit exposed was a recent sand deposit that filled the depression that is visible in the air photo. This sand deposit thins dramatically to the southwest across Fault A, indicating that there was a small scarp present at the time of the photo, which most likely caused the ponding of water (Figure 2). Older stratigraphic relationships seen in the trench repeat this pattern and indicate that this sag forms during ruptures along Fault A and then slowly fills with sediment from the badlands to the north and east. Evidence for this exposed in the trenches included vertical separation across Fault A in the form of faulted sediments, folding, angular unconformities, and units thinning to the southwest against paleoscarps. A secondary fault zone (which we consider part of Fault A) is located about 20 m to the southwest and only the older events were preserved along this fault zone in the trenches. The younger events are not well expressed in this secondary fault zone because the secondary fault zone is on the up-thrown side of the main fault and the younger stratigraphy is drastically thinned or eroded off on the southwest side of the main fault zone. There is a lesser degree of vertical offset along the faults in the secondary fault zone and all of the events seen in the secondary fault zone are also seen in the main fault zone where the trenches were deep enough to expose the same stratigraphic level. The three oldest events we observed in the trench exposures were in the secondary fault zone. We expect that these events are also present in the main fault zone, and probably better expressed, but are at a deeper level than the trenches were excavated.

Trenches excavated across Faults B and C (Figure 2) provided evidence that these faults are not as active as Fault A and are probably older. The only evidence for movement along these faults in the past 2000 years was a single fault that cut sediments dated 1990 ±20 rcyBP at 2 m depth in Trench 4 across Fault C. Faults in Trench 3 across Fault B cut sediments dated 8645 ±45 rcyBP.

No younger sediments were present in either Trench 3 or 4 with which to evaluate an upper bound for these faults. No trenches were excavated across Fault D because the fault is interpreted to be pre-Holocene based on the fact that it does not deflect younger drainages and is covered by unfaulted older alluvium in an outcrop .5 km to the southeast.

Event evidence

Evidence for surface rupture at the site included upward terminations of multiple faults at the same stratigraphic level, filled fissures, folding of strata across the main fault zone, and associated onlap of stratigraphic layers and angular unconformities (Figures 3, 4, 5, and 6). A stratigraphic pattern is present that indicates the geomorphic changes and depositional response at the site due to repeated surface ruptures. Most event horizons occur at the top of fine-grained, dark organic layers that we interpret to be paleosols that represent periods of quiescence and soil formation. These event horizons are overlain by lighter clay or silty clay deposits that are not tilted as much as the underlying organic horizons and thin as they approach and cross the main fault zone. We interpret these relationships to be the result of subsidence of the sag during each surface rupture at the site. The rupture faults and/or folds the soil that existed at the surface at the time of the earthquake and then the sag slowly fills with sediment. A soil then develops on the new sediments until the next earthquake causes renewed subsidence. Figures 3, 5 and 6, show the alternating light layers (sag fill sediments) and dark layers (organic paleosols) and the folding that occurs across the main fault zone exposed in the deeper trenches funded by this study (Trenches 8 and 9). Figure 4 shows typical relationships in the secondary fault zone in Trench 8, where the folding and faulting is less pronounced. No trench logs from the shallow trenches (Trenches 1 through 7) are included in this report because of limited space, and because these trenches and the relationships exposed in them are described in detail in Onderdonk et al. (2013), which is included with this grant report. Table 1 below summarizes the event evidence from all trenches excavated at the Mystic Lake site across the primary fault strand.

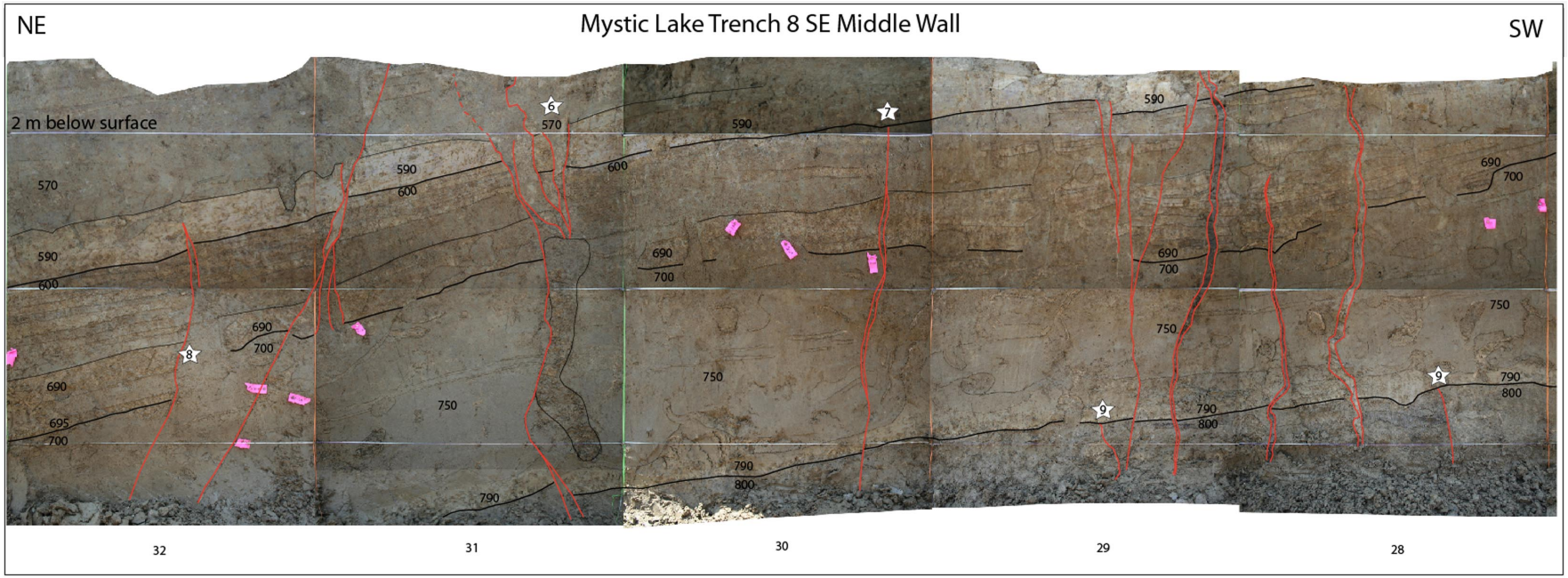

Figure 3. Photomosaic of the main fault zone exposed in Tier 2 on the southeast wall of Trench 8. Key stratigraphic units are bounded by black lines and faults are shown a red lines with white stars denoting the evidence for events. Dark organic layers interpreted to be paleosols (Units 600, 700, 800) are present below the event horizons, and lighter silty clay layers (590, 690, 790) are present directly above the event horizons. Note the folding across the fault zone as the layers are dropped downward to the northeast into the sag.

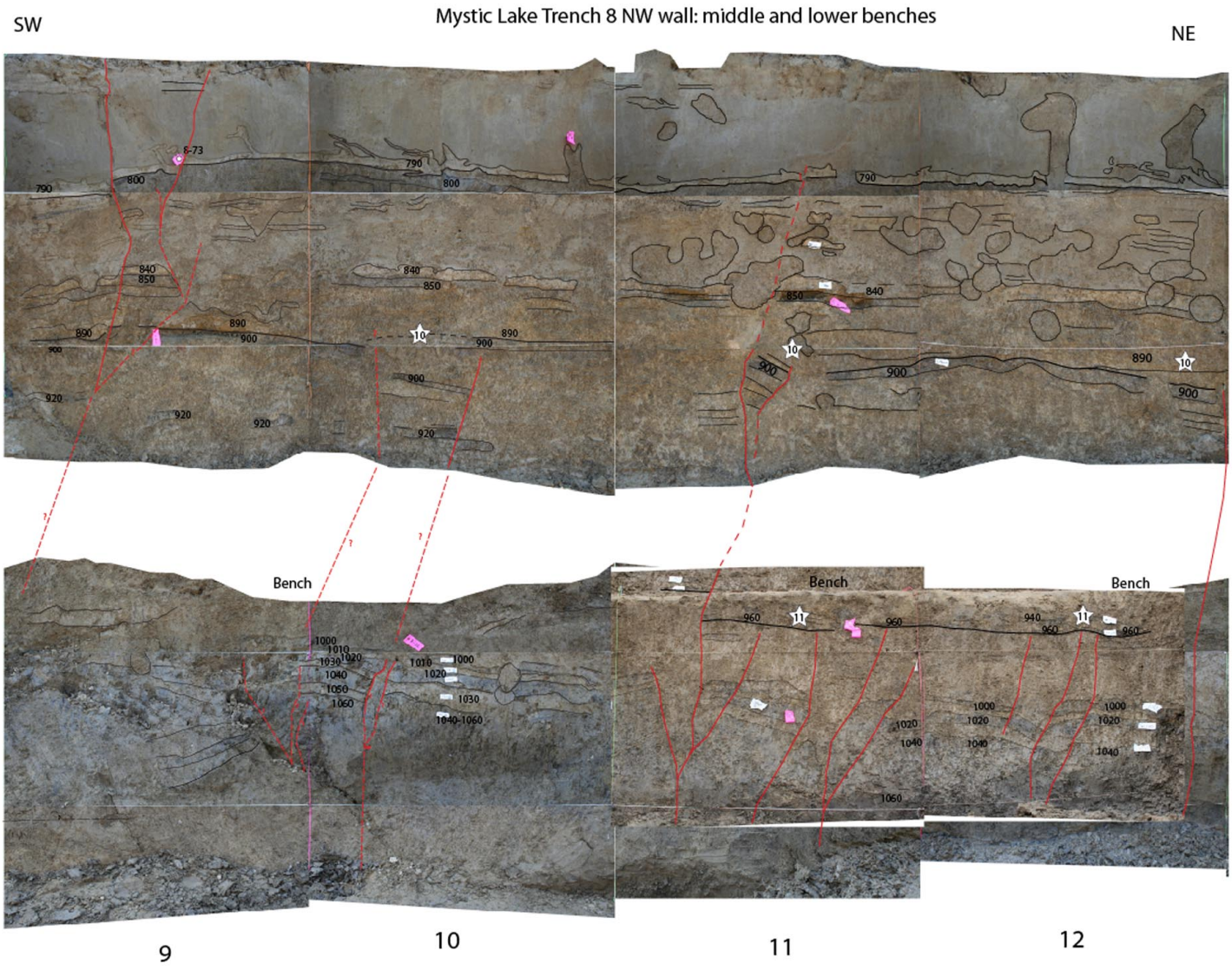

Figure 4. Photomosaic of Tiers 2 and 3 on the northwest wall of Trench 8 showing selected stratigraphic units (bounded by thin black lines), faults (subvertical red lines), and event horizons (white stars with event number). These panels are from the secondary fault zone that is present about 20 m to the southwest of the main fault zone where older stratigraphy is exposed due to relative uplift of the southwest side of the fault.

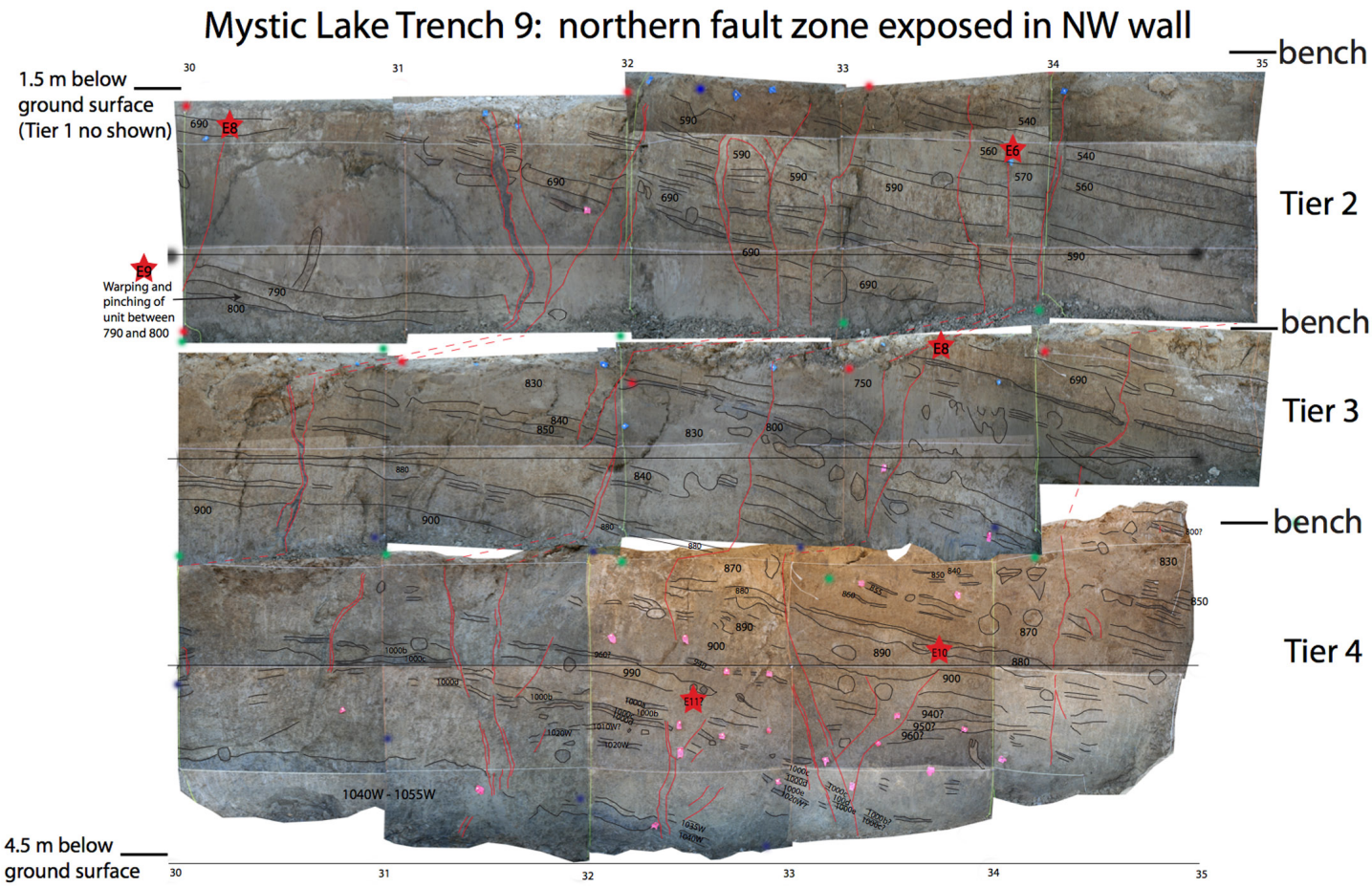

Figure 5. Photomosaic of Tiers 2, 3, and 4 on the northwest wall of Trench 9 showing stratigraphic contacts (thin black lines), unit labels (black numbers), faults (subvertical red lines), and event horizons (red stars).

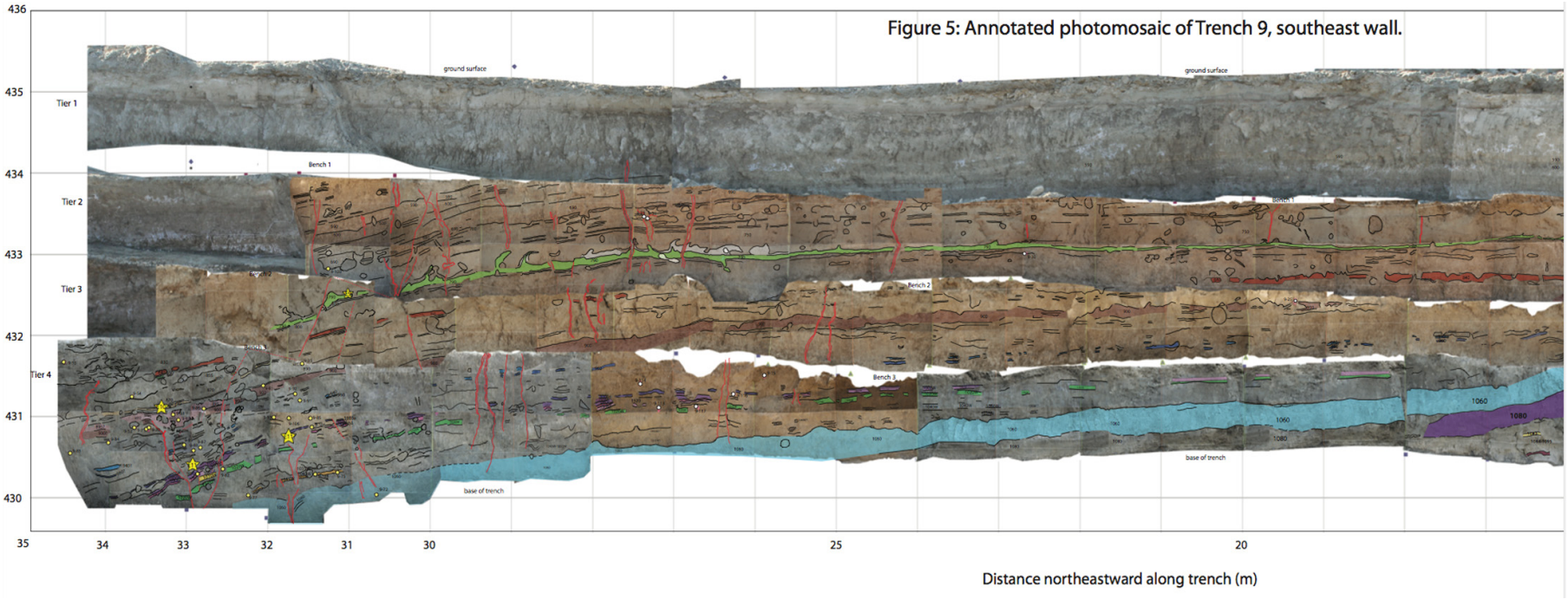

Figure 6. Photomosaic of part of the southeast wall of Trench 9 (all tiers) showing faults (red lines), and selected stratigraphic contacts (thin black lines). Unit 1060 is colored light blue to highlight the folding that and thickening that occurs across the main fault zone. Also note the thinning of units to the southwest and the increased tilted with stratigraphic depth in the northeaster part of the trench.

Table 1. Summary of Evidence for Earthquakes at Mystic Lake from T1, T6, T7, T8, T9

Event	Unit	Exposure	Evidence	Confidence
E0	Top of 10 and possibly higher	T1 M52	Thickening of the sand layer across the fracture zone into the sag and folding of Unit 10.	Strong
		T7 M13	Faults offset Unit 10 with 1- 3 cm down to the northeast separation and may extend up into Unit 1. Upward termination of fractures. Thickening of the sand layer across the fracture zone into the sag.	Strong
		T6 M17	Faults offset Unit 10 with down to the SW displacement.	Strong
E1	Top of 100	T1 M52,53	Upward termination of two clay seams with down to the SW displacement.	Strong
		T1 M17, 33	Faults cut Unit 200 and are lost in Unit 100.	Weak
		T1 M76	Upward termination of fault.	Strong
		T6 M14,15 nwM13,15	Upward termination of faults with down to the NE displacement.	Strong
		T7 M13,14,15	Upward termination of numerous fractures without resolvable displacement and one or two faults that appear to disrupt two white silt layers within Units 100-200.	Moderate
E2	Top of 200	T1 M59 east	Upward termination of a fault, fissure fill.	Strong
		T1 M18	Upward termination of a fault. SW side down.	Strong
		T1 M72	Upward termination of faults.	Strong
		T1 M77	Upward termination of a fault.	Strong
		T6 nwM16,17	Upward termination of faults.	Strong
E3	Top of 300	T1 M33	Upward termination of faults. NE side down.	Strong
		T1 M45-53	Folding of Units 300 and below across the SW fault zone.	Strong
		T7 M12	Upward termination of faults that define a graben.	Strong
		T7 M7-12	Folding of Units 300 and below truncated by an angular unconformity at the base of Unit 250. Onlap and pinching of Units 290, 270 against a fold scarp.	Strong
E4	Top of 400	T1 M50,51	Upward termination of faults.	Strong
		T1 M45-51	Thinning and pinching of units 300 – 400 against the E4 fold scarp.	Strong
		T6 M14	Upward termination of faults.	Strong
E5	Top of 500	T1 M51	Upward termination of faults.	Strong

		T1 M45-54	Thinning of units above the event horizon across the faults.	Strong
		T6 M14	Upward termination of fault.	Strong
		T6 M16, 17	Possible upward termination of faults.	
E6	Top of 570	T1 M51,52,53	Upward termination of faults.	Strong
		T1 M53	Possible fissure fill.	Weak
		T6 M14	Warping of strata against the fault.	Strong
		T6 M18	Upward termination of faults.	Strong
		T7 M31SE 2nd tier, and M30-31 SE 1st tier	Unit 590 is offset, forming a graben that extends down into Unit 750. Unit 570 is filling the graben. Unit 560 is not offset, but is discontinuous across the top due to bioturbation. Infer Unit 560 to be unfaulted.	Moderate
		T9 M34 NW Tier 2	Fault cuts Unit 570 and below (down 8 cm on NE side) but does not cut the base of Unit 560	Weak
E7	Top of 600	T1 M53	Upward termination of fault.	Strong
		T1 M54	Upward termination of fault.	Strong
		T1 M73	Upward termination of faults.	Strong
		T8 M30 SE Tier 2	790/800 is clearly offset and Unit 750 is filling in graben from above. Unit 690 offset 2cm down on the NE, but Unit 590 does not look offset.	Moderate
E8	Top of 700	T8 M32 SE Tier 2	Unit 690 thickens across a fault from 8 to 10 cm on the SW to about 20 com on the NE with some sand mixed in that probably come off the scarp. The 690/700 contact is offset about 25 cm down on the NE side, while the upper contact of Unit 690 is only offset about 10 cm (by a later event that goes up through Unit 590 and offsets units between 690 and 590 by about 5 to 7 cm)	Strong
		T8 M32 NW Tier 2	Unit 690 thickens across a fault that offsets Unit 790 about 3 to 4 cm down on the NE side. An adjacent fault offsets the base of Unit 690 about 10 cm, while the top of 690 is only offset about 5 to 6 cm. A third fault cuts or warps Unit 700, but Unit 690 does not look offset.	Strong
		T9 M31 NW Tier 2	Fault cuts Unit 790 and below, hard to trace through 700's but does not cut Unit 690	Strong
		T9 M34 NW Tier 3	Fault cuts Unit 750 and below, but doesn't cut Unit 690	Weak (could merge with adjacent fault)
E9	Top of 800	T8 M29 SE Tier 2	Clay seam that offsets deeper layers is truncated at the base of Unit 790	Strong
		T8 M28 SE Tier 2	Fault that offsets deeper layers is truncated at the base of Unit 790	Strong

		T8 M13 SE Tier 2	Fault offsets units 820, 840 and below (3 cm down to the NE), but is truncated at the base of Unit 790	Strong
		T8 M32 SE Tier 3	Fault offsets Unit 800 and below down 4 cm on the NE side, but does not cut Unit 790. Unit 790 thickens across the fault.	Strong
		T9 M27 SE Tier 2	Fissure fill. Unit 790 dropping into a fissure in Unit 800, which is offset 5 cm on NE side	Strong
		T9 M32 SE Tier 3	Offset units below Unit 800 (up on NE side) but units 790 and 800 don't look offset	Weak (faults can't be followed downward)
		T9 NW wall Tiers 2 and 3	Warping and pinching of fine-grained layer between units 790 and 800	Strong
E10	Top of 900	T8 M10 NW Tier 2	A graben drops Unit 900 down, but units 850 and 840 are not disturbed and Unit 890 seems to go across the fault undisturbed as well	Weak
		T8 M12 NW Tier 2	Unit 900 sags down, while Unit 890 goes straight across	Strong
		T8 M11 NW Tier 2	Unit 900 is tilted down between two faults. The fault on the right is capped by Unit 890. The fault on the left goes up higher through Unit 790	Strong
		T8 M29 SE Tier 3	Unit 900 is offset by a fault, but Unit 890 drapes across and units 840, 850 go right across	Moderate
		T8 M26 NW Tier 3	Fissure develped in Unit 900 and below. Unit 890 fills the tissue and drapes across.	Strong
		T9 M34 NW Tier 4	Fissure cuts Unit 900 and below (down 10 cm on SW side), filled by Unit 880, which drapes across	Strong
		T9 M33 SE Tier 4	Fissure cuts Unit 900 and below (down 10 cm on SW side), filled by Unit 880, which drapes across	Strong
E11	Top of 970	T8 M10 NW Tier 3	Faults cut and tilt Unit 990 and below, but do not cut Unit 960	Strong
		T8 M11 NW Tier3	Faults cut and tilt Unit 990 and below, but do not cut Unit 960	Strong
		T8 M12 NW Tier 3	Faults cut and tilt Unit 990 and below, but do not cut Unit 960	Strong
		T9 M33 SE Tier 4	Units cut under Unit 1030 sand but Unit 1030 sand and dark layer above warp across, then a clay layer covers it all and thickens across the fault (Unit 100c)	Moderate
		T9 M32 SE Tier 4	Fissure that is capped around the stratigraphic level of Event 11 (Unit 1000 in T9 main fault zone)	Weak
		T9 M33 NW Tier 4	Fissure that ends upward around Unit 1000b (clay that also fills the fissure?)	Weak

E12	Top of 1060	T9 Whole trench	Units between 1060 and 1020 pinch out against 1060 from NE to SW. 1060 is tilted more than units above. Strong tilt at M16 and another strong warp (possibly offset) at M24	Strong
E13	Base of 1060 or within 1070	T9 M11-13 SE Tier 4	Unit 1082 offset 10 cm down to NE, base of Unit 1060 not cut. Faults extend down into a graben at depth that does not affect Unit 1060	Moderate
E14	Base of 1090	T9 M14 NW Tier 4	Unit 1200 is offset 10 to 15 cm down to the NE, Fissues in Unit 1150, but base of 1090 is not cut.	Strong
		T9 M12 NW Tier 4	Fractures cut up through Unit 1150, but do not cut Unit 1090	Moderate
E15	Base of 1150	T9 M10 NW Tier 4	Top of Unit 1200 is offset, but the top of Unit 1200 does not continue to the faults that define the next higher event (14) suggesting that a fissure existed in Unit 1200 before Unit 1150 was deposited. Also a thin clay layer that drapes across the offset Unit 1200, and this clay layer is offset by E14 faults.	Weak

Earthquake Record

The trenches exposed evidence for 15 ground-rupturing earthquakes at the Mystic Lake site and the timing of these events was determined using radiocarbon dates collected from stratigraphic units above and below event horizons. OxCal software (Bronk Ramsey, 2009) was used to compute probability density functions for each event (Figure 7). A significant amount of time is present in our model between Events 12 and 13 (Figure 8). We infer that this is due to missing stratigraphy in the deeper part of Trench 9 where these events were exposed. Events 13, 14, and 15 were only exposed in the secondary fault zone at the southwest end of Trench 9 where older stratigraphy is present at shallower depths. These events are present below Unit 1060 (shown in blue in Figure 6), which is tilted and drops below the deepest part of the trench in the main fault zone to the northeast. Radiocarbon samples within Unit 1060 span almost 700 years (Appendix 1) and there is an angular unconformity at the top of Unit 1060 that we infer to represent Event 12. We infer that Event 12 lifted the southwest side of the fault causing erosion of at least 700 years of stratigraphy. This stratigraphy may be preserved in the main fault zone, but if so, it is deeper than the 4.5 m depth of Trench 9. Deeper trenching would most likely provide evidence for addition events between Events 12 and 13, as well as older events, but this was beyond the time and funding allotted for this study. Deeper trenching should be considered at the site, although we found that wetter conditions at depth required substantially more effort to keep the trench walls from collapsing and the stratigraphy seemed to be poorly defined in the deepest 2 meters of the main fault zone.

We have a complete record for the last 2000 years, during which there were 12 ground rupturing earthquakes at the Mystic Lake site (Figure 8). The recurrence interval for this period is about 175±20 years. The last earthquake at the site occurred sometime after AD 1740. We assume an

upper bound of AD 1850 for this event because the historic record in the area extends back to this time and does not include a major ground rupturing earthquake on the Claremont fault. The penultimate earthquake (E2) has a double peak with the younger peak being centered around 1800. But paleoseismic data from the Quincy site about 11 km to the northwest on the Claremont fault (Onderdonk et al., in review), narrows the time range for E2 to the earlier peak if we assume both sites experienced the same events in the last few hundred years. The elimination of the younger peak of Event 2, causes the peak in the PDF of Event 1 to be centered around 1800, which is close in time to two large earthquakes recorded in mission records in the region (Toppazada et al., 1981). Assuming 1800 as the approximate age of Event 1 means it has been about 200 years since the last ground-rupturing earthquake on the Claremont fault. This is roughly equal to or longer than the recurrence interval of 175±20 years, which suggests the Claremont fault is near the end of its earthquake cycle. The coefficient of variation for the last 2000 years at the Mystic Lake site is .4, which suggests that earthquakes are fairly regular and thus raises the likelihood of a rupture in the near future.

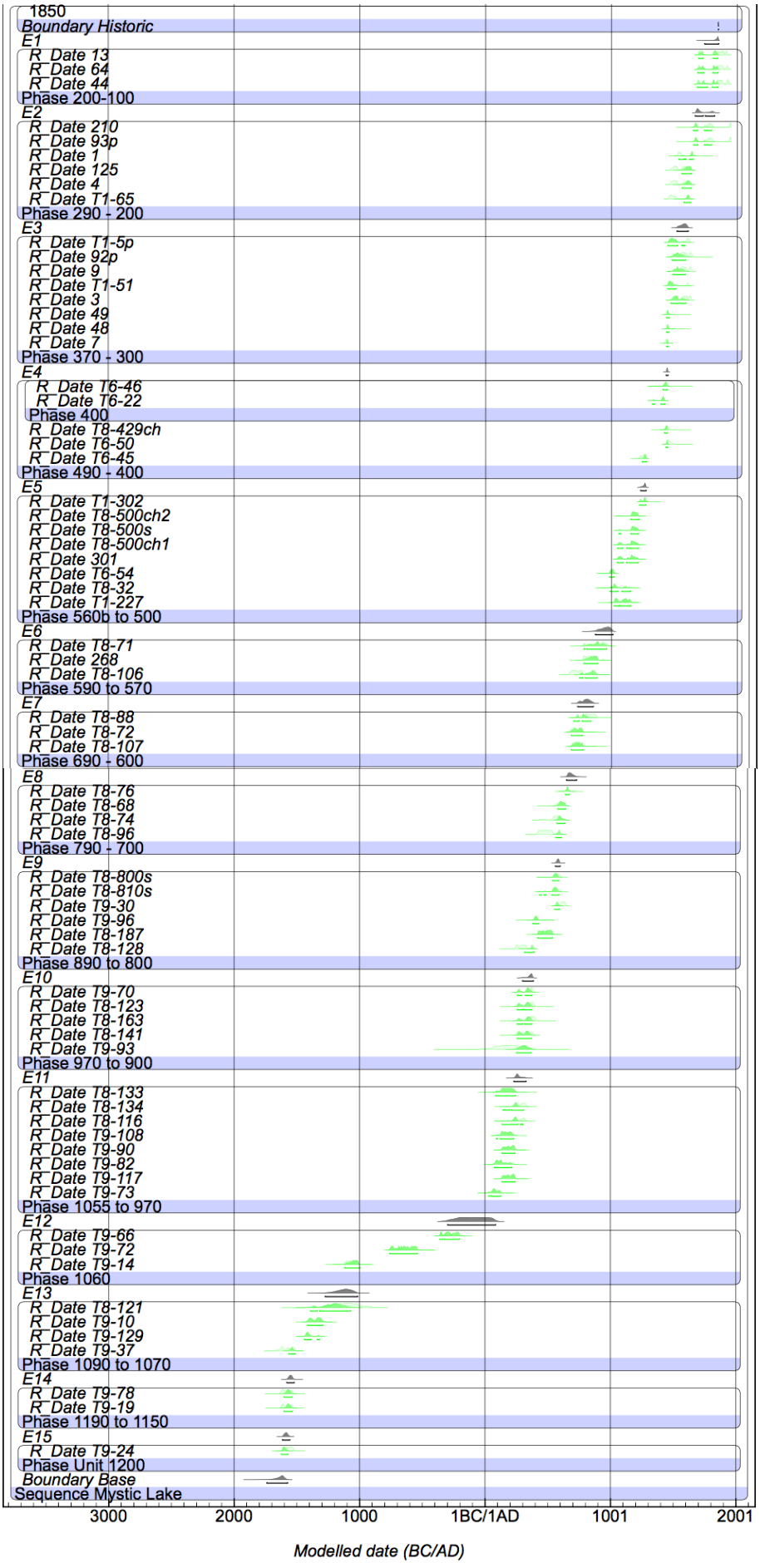

Figure 7. OxCal model of the Mystic Lake stratigraphy. Radiocarbon ages are show as green PDFs and earthquake ages are show as black PDFs.

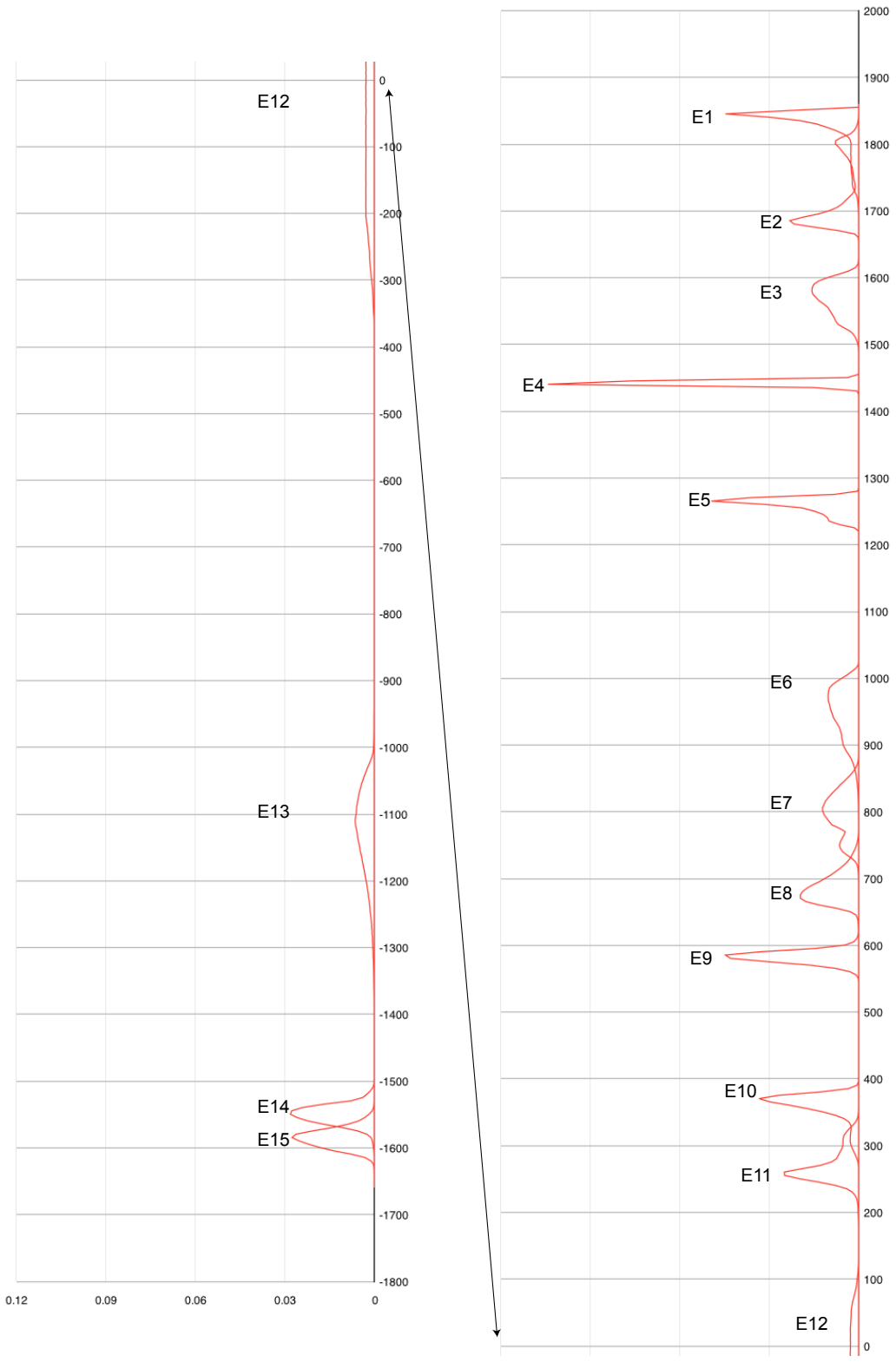

Figure 8. Event history for the Mystic Lake site with earthquake ages represented as PDF curves (red lines).

Recent data from the Quincy site on the Claremont fault (Onderdonk et al., in review) suggests a slip rate for the fault of 12 to 19 mm/yr. This implies that about 2.5 to 3.8 m of slip has accumulated on the fault, assuming an average age of AD 1800 for the last earthquake. These numbers roughly agree with estimates of 2.3 to 3 m average slip per event for the last 9 to 12 earthquakes at the Quincy site (Onderdonk et al., in review).

Comparisons with the Hog Lake and Wrightwood paleoseismic records

Comparison of the Mystic Lake event history with those from the Hog lake site on the central San Jacinto fault zone to the southeast (Rockwell et al., in press), and the Wrightwood site on the Mojave section of the San Andreas fault to the northwest (Fumal et al., 2002), shows overlaps in the timing of some events (Figure 9). The most recent event at Mystic Lake occurred sometime between AD 1740 and AD 1850 and overlaps in time with events at both the Hog Lake and Wrightwood sites. We explore the two possible correlations here. Rockwell et al. (2004) and Salisbury et al. (2012) interpreted the penultimate earthquake at the Hog Lake site (HL2 in Figure 9) to be the Nov. 22 1800 earthquake that caused extensive damage at the San Juan Capistrano and San Diego missions (Toppazada et al., 1981). If Event 1 at Mystic Lake is the same earthquake, this implies that the earthquake ruptured through the releasing step-over between the Claremont and Casa Loma- Clark faults. An alternative possibility is that the 1812 earthquake on the Mojave section of the San Andreas fault recorded at the Wrightwood paleoseismic site also ruptured the northern San Jacinto fault southeast to the Mystic Lake area. This interpretation requires that the earthquake ruptured through the step over at the northern end of the Claremont fault rather than continuing down the San Bernardino segment of the San Andreas fault. The available paleoseismic data from this segment of the San Andreas fault are conflicting with respect to the timing of the last event and cannot be used to definitively confirm the southern extent of the 1812 rupture. Data from the Plunge Creek site on the San Bernardino segment indicate that the last rupture occurred prior to AD 1730 (McGill et al., 2002), but interpretations from the Burro Flats site in the San Gorgonio Pass area, and the Pitman Canyon site just south of the Cajon Pass favor a scenario where the 1812 earthquake ruptured the San Bernardino segment of the San Andreas as far south as the San Gorgonio Pass (Seitz et al., 1997; Yule and Seih, 2001). A third possibility is that the most recent event at Mystic Lake was a separate earthquake that occurred close in time to the 1800 and 1812 events.

There are four events at the Mystic Lake site that overlap in time with events at Hog Lake (Rockwell et al., in press). These possible correlations suggest that some events on the San Jacinto fault rupture through the step-over between the Claremont fault and the Casa Loma-Clark fault. Marliyani et al. (2013) presented cone penetrometer data and geomorphic observations from the Mystic Lake site and the surrounding area that suggest this step over has narrowed over time due to development of younger faults in the step over. Considering the possible hard link proposed by Marliyani et al. (2013), and the relatively narrow width of the step-over (less than 1 km at the north end), we consider rupture through the step-over to be a possibility. This scenario would enable ruptures on the San Jacinto fault zone to extend 145 km or more, which corresponds to a Magnitude Mw 7.7 or larger earthquake (Wells and Coppersmith, 1994) and would help explain the significant destruction of missions along the

coast in the Nov. 22 1800 earthquake. The alternative explanation is that these overlapping ages are just closely timed earthquakes on the separate faults.

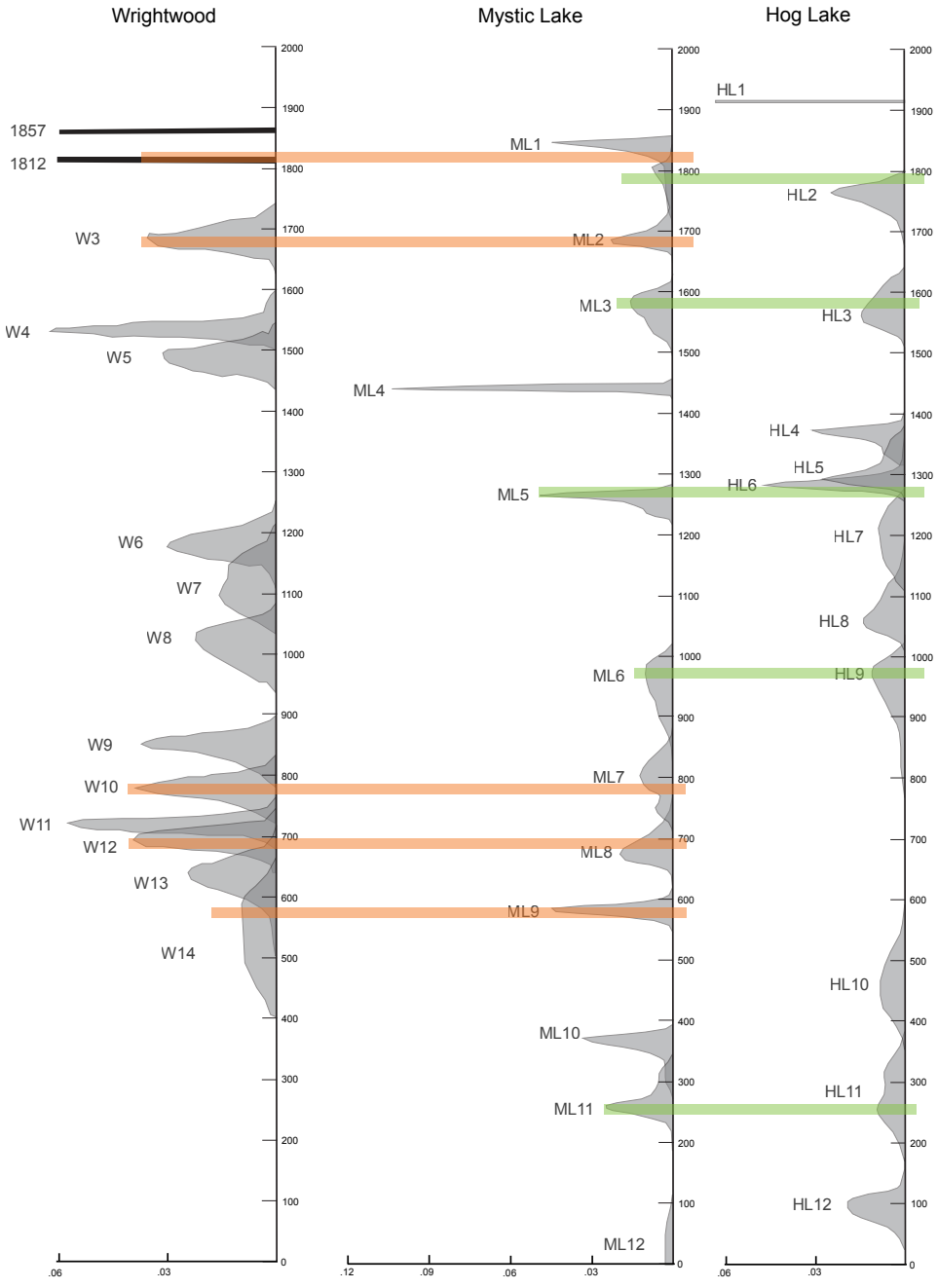

Figure 9. Comparison of event ages from the Wrightwood, Mystic Lake, and Hog Lake paleoseismic sites. Event PDFs are shown in gray for each site and possible correlations are shown as green or orange lines.

There are also four events at the Mystic Lake site that overlap in time with events recorded at the Wrightwood site (Fumal et al., 2002). If these correlations are real, then some earthquakes have ruptured through the step-over between the northern end of the San Jacinto fault and the San Andreas fault in the Cajon Pass area. This step-over is also less than 1 km wide, which is well below the 4 km threshold width for ruptures across a step-over proposed by Wesnousky (2006) based on historic ruptures. Further work, in the form of mapping ruptures in the topography or better resolution dating of the events, would be needed to confirm these possible correlations. It is interesting to note that none of the events shown on Figure 9 can be correlated between all three sites, suggesting that a rupture from the Clark fault to the Mojave section of the San Andreas fault is not possible. It is also interesting to note that if ALL of the possible correlations shown on Figure 9 are correct, all but one earthquake on the Claremont fault in the past 2000 years has occurred in conjunction with rupture on either the San Andreas fault, or the central San Jacinto fault.

Conclusions

The new paleoseismic data generated by this study indicate that the Claremont fault has experienced 11 or 12 large, ground-rupturing earthquakes in the last 2000 years. The data also show that the most recent ground rupture event was about 200 years ago, which is longer than the average recurrence interval of 175 ± 20 years. Comparison of the timing of events documented at the Mystic Lake site with other paleoseismic data on the central San Jacinto and the San Andreas fault suggest that some earthquakes have ruptured through the step-overs at the northern and southern end of the Claremont fault, thereby increasing the expected magnitude of earthquakes on this fault.

Work Cited

Bevis, M., K. Hudnut, D. Brzezinska, R. Sanchez, and C. Toth (2006). The B4 LiDAR survey of the southern San Andreas and San Jacinto faults, *Seismol. Res. Lett*. **77**, 311.

Bronk Ramsey, C. (2009). Bayesian analysis of radiocarbon dates, *Radiocarbon* **51**, 337-360.

Fumal, T.E., R. J. Weldon, II, G. P. Biasi, T. E. Dawson, G. G. Seitz, W. T. Frost and D. P. Schwartz, (2002). Evidence for large earthquakes on the San Andreas fault at the Wrightwood, California, Paleoseismic site: A.D. 500 to present, *Bull. Seis. Soc. Am*. **92** 2726-2760.

McGill, S., S. Dergham, K. Barton, T. Berney-Ficklin, D. Grant, C. Hartling, K. Hobart, R. Minnich, M. Rodriguez, E. Runnerstrom, J. Russell, K. Schmoker, M. Stumfall, J. Townsend, and J. Williams, (2002). Paleoseimology of the San Andreas fault at Plunge Creek near San Bernardino, southern California. *Bull. Seism. Soc. Am*, **92** 2803-2840.

Reimer, P. J., Baillie, M. G. L., Bard, E., Bayliss, A., Beck, J. W., Blackwell, P. G., Bronk Ramsey, C., Buck, C. E., Burr, G. S., Edwards, R. L., Friedrich, M., Grootes, P. M., Guilderson, T. P., Hajdas, I., Heaton, T. J., Hogg, A. G., Hughen, K. A., Kaiser, K. F., Kromer, B., McCormac, F. G., Manning, S. W., Reimer, R. W., Richards, D. A., Southon, J. R., Talamo, S., Turney, C. S. M., van der Plicht, J., & Weyhenmeyer, C. E. (2009). IntCal09 and Marine09 radiocarbon age calibration curves, 0-50,000 years cal BP, *Radiocarbon* **51**(4), 1111-1150.

Rockwell, T. K., G. Seitz, T.E. Dawson, and J.J. Young (*in revision*). A 4000 year record of surface ruptures along the central San Jacinto fault at Hog Lake: Implications for earthquake recurrence and fault interaction models. *Bull. Seism. Soc. Am.*

Rockwell, T., G. Seitz, J. Young, and T. Dawson (2004). Late Holocene earthquake history of the Anza seismic gap, central San Jacinto fault zone, southern California. Final Technical Report for USGS Grant No. 04-HG-GR-0083.

Salisbury J. B., T. K. Rockwell, T. J. Middleton, and K. W. Hudnut (2012). LiDAR and field observations of slip distribution for the most recent surface ruptures along the central San Jacinto fault. *Bull. Seism. Soc. Am.* **102** 598-619.

Seitz, G., R. Weldon, and G. Biasi, (1997). The Pitman Canyon paleoseismic record: a re-evaluation of southern San Andreas fault segmentation, *Journal of Geodynamics* **24** 129-138.

Wells, D. and K. Coppersmith (1994). New empirical relationships among magnitude, rupture length, rupture width, rupture area, and surface displacement, *Bull. Seism. Soc. Am.,* **84** 974-1002.

Yule, D. and K. Seih, (2001). The paleoseismic record at Burro Flats: Evidence for a 300-year average recurrence for large earthquakes on the San Andreas fault in San Gorgonio Pass,

southern California, *Geol. Soc. Am. Abstracts with Programs- Cordilleran Section Meeting (April)* **33**(3) 31.

Publications that include data from this project

Onderdonk, N.W., McGill, S.F., and T.K. Rockwell, in review, Late Holocene rate of lateral slip and size of pre-historic earthquakes on the northern San Jacinto fault zone during the past 2000 years. Submitted to Lithosphere.

Rockwell, T. K., G. Seitz, T.E. Dawson, and J.J. Young, in revision. A 4000 year record of surface ruptures along the central San Jacinto fault at Hog Lake: Implications for earthquake recurrence and fault interaction models. *Bull. Seism. Soc. Am.*

Onderdonk, N.W., T.K. Rockwell, S. F., McGill, and G. I. Marliyani (2013). Evidence for seven surface ruptures in the past 1600 years on the Claremont fault at Mystic Lake, northern San Jacinto fault zone, California, *Bull. Seismol. Soc. Am*. **103**, no. 1, 519-541

Marliyani, G. I., T. K. Rockwell, N. W. Onderdonk, and S. F. McGill (2013). Straightening of the northern San Jacinto Fault, California as seen in the fault-structure evolution of the San Jacinto Valley stepover. *Bull. Seismol. Soc. Am*. **103**, no. 3. doi: 10.1785/0120120232

Appendix 1: Radiocarbon Dates

Appendix 1: Radiocarbon Dates

Mystic Lake, San Jacinto fault. Model 4 (PREFERRED)					
Gray shading indicates samples that were not used in OxCal mode					
Events	**Unit**	**sample #**	**trench panel**	**C-14 age**	**1 sigma**
Event 0	1				
	10	238	63	modern	
Event 1	Top of 100				
	100-200	T7-13	18	105	15
	100-200	T6-64	17	120	15
	100-200	T7- 44	18	130	15
	100-200	T7- 43	5	620	15
	100	T7-26	15	1740	90
	190	T1- 214	16	355	20
Event 2	Top of 200				
	200	T1- 219	33	40	20
	200	T1- 7	E1	370	20
	230	T1- 210	16	195	20
	240	T1- 55	E20	300	20
	250	T1- 93p	E57	195	20
	270?	T7- 1	2	295	15
	290	T1- 220	34	670	90
	290	T1- 125	E67	345	20
	290	T7- 4	4	355	20
	290	T1- 65	E27	375	20
	290	T1- 208	16	625	20
Event 3	Top of 300				
	300	T1- 5p	E1	370	20
	310	T1- 221	34	820	20
	320	T1- 92p	E56	325	20
	320-340	T7- 9	9	325	15
	340	T1- 51	E20	390	20

Mystic Lake, San Jacinto fault. Model 4 (PREFERRED)					
	360?	T7- 3	3	340	15
	370	T1- 212	17	1310	20
	370	T1- 209	16	1095	20
	370	T1- 226	49	865	20
	370	T6- 49	12	440	15
	370	T6- 48	12	445	15
	370	T6- 52	14	1210	15
	390	T7- 7	11	475	15
Event 4	Top of 400				
	400	T6-22	8	545	15
	400	T6- 25	8	1120	15
	400	T8-400s		320	15
	400	T6- 46	11	480	30
	420	T8-420ch		460	20
	430?	T6- 50	12	410	15
	450?	T6- 42	11	1310	60
	480?	T6- 45	11	785	15
	480	T8-33	SE_M_33	1105	20
	400	T1- 244	67	(-890)	90
Event 5	Top of 500				
	500-520	T1-302	50	740	15
	500	T8-500ch1		885	20
	500	T8-500ch2		870	15
	500	T8-500s		875	15
	500	T1- 301	50	890	20
	520	T6- 61	16	1240	15
	530	8-66		1140	25
	530?	T6- 54	14	1045	15
	540	T6- 60	16	1120	15
	540	8-32		995	30
	540-500	T6-53	14	2080	60
	550	T8-81	SE_M_34	1200	20
	560a	T6- 55	14	2160	80
	560a	T6- 56	14	1185	15
	560	8-85		Died in pretreatment	
	560?	T1- 227	50	960	25

Mystic Lake, San Jacinto fault. Model 4 (PREFERRED)					
Event 6	Top of 570				
	570	T8-71	NW_M_35	1150	25
	580?	T1- 268	79	1185	20
	580	T1- 232	60	modern	
	590	8-58		-3580	150
	590	T8-106	SE_M_30	1280	35
Event 7	Top of 600				
	600	T8-88	NW_M_36	1205	20
	600	T9-137	NW Tier 2 33-34	1600	20
	600	T9-140		-4030	100
	600	T1- 254	68	1470	30
	620	8-72		1280	25
	640 to 680	8-62		1580	25
	640	T9-133	NW Tier 2 33-34	1620	40
	650 to 680	8-108		1435	25
	650 to 680	8-107		1260	25
	690	8-90		Died in pretreatment	
	690	8-37		1520	25
	690	8-100		1550	25
	670	T9-138		1980	30
	690	T9-139		1545	15
	690	T1- 230	55	1550	20
	690	T8-93	NW_M_31	1720	20
	695	T8-89	NW_M_32	1505	20
Event 8	Top of 700				
	700	T8-76	SE_M_31	1365	20
	700	T1- 234	60	1685	25
	700	T1- 235	62	1725	20
	700	T9-97	NW Tier 2 31-32	2720	150
	710	T8-68	SE_M_28	1460	20
	710	8-47		1910	25
	730	8-95		Died in pretreatment	
	750	8-28		Died in pretreatment	
	750	T8-79	SE_M_32	1995	20
	750	T1- 239	63	(-1105)	35
	760	8-74		1500	30

Mystic Lake, San Jacinto fault. Model 4 (PREFERRED)					
	790	8-96		1575	25
	790	T9-135		1910	40
	790	T9-94	NW Tier 3 32-34	1725	30
	790	T8-191	SE_L_32	2390	60
	790	T8-153	SE_L_31	2040	40
Event 9	Top of 800				
	800	T1- 250	67	1705	25
	800	T8-800s		1500	15
	810	T8-810s		1510	20
	820	T9-30	SE Tier 2 22-23	1445	15
	850	T9-96	NW Tier 4 33-34	1640	15
	850	T8-187	SE_M_29	1580	20
	880	T9-35	SE Tier 4 31-32	3320	70
	890	T8-128	NW_M_11	1755	20
Event 10	Top of 900				
	910	T9-70	SE Tier 4 33-34	1705	15
	910	8-123		1705	25
	920	8-163		1685	30
	940	8-181		Died in pretreatment	
	940	T9-60	NW Tier 4 32-33	1880	15
	940	T9-88	SE Tier 4 32-33	1805	15
	950	T8-141	SE_L_12	1720	20
	960	T9-93	SE Tier 4 31-32	1830	90
	960	T8-140	SE_L_12	2150	60
Event 11	Top of 970				
	970	T8-133	SE_L_13	1835	35
	970	T8-134	SE_L_13	1770	20
	990	T8-116	NW_L_10	1780	20
	990	T9-108	NW Tier 4 32-33	1850	15
	1000c	T9-90	SE Tier 4 32-33	1815	15
	1000	T8-1000ch		2100	15
	1020	T9-55	NW Tier 4 30-31	2210	15
	1020w	T9-82	SE Tier 4 32-33	1875	20
	1020	T9-117	SE Tier 4 26-27	1815	15
	1055w	T9-73	SE Tier 4 31-32	1925	20

Mystic Lake, San Jacinto fault. Model 4 (PREFERRED)					
Event 12	Top of 1060, Bottom of 1055				
	1060	T9-66	NW Tier 4 31-32	2210	15
	1060	T9-72	SE Tier 4 30-31	2480	15
	1060	T9-14	NW Tier 4 14-15	2885	20
Event 13	Top of 1070, bottom of 1060				
	1080	T9-126	NW Tier 4 11-12	3380	15
	1082	T9-26	SE Tier 4 12-13	3150	15
	1090	T8-121	NW_L_6	2920	70
	1090	T9-10	SE Tier 4 15-16	3090	20
	1090	T9-129	NW Tier 4 13-14	3130	15
	1095	T9-37	NW Tier 4 13-14	3320	20
Event 14	Top of 1150, Below 1090				
	1150	T9-20	NW Tier 4 11-12	3810	60
	1150	T9-78	NW Tier 4 11-12	3310	20
	1190	T9-19	NW Tier 4 11-12	3310	15
Event 15	Below 1190, Above 1200				
	1200	T9-24	SE Tier 4 10-11	3290	15
	1200	T9-12	NW Tier 4 9-10	3525	20
	1200	T9-29	NW Tier 4 11-12	4040	60